X-ray Absorption Spectroscopic Study on the Electronic Structure of $Li_{1-x}CoPO_4$ Electrodes as 4.8 V Positive Electrodes for Rechargeable Lithium Ion Batteries

Masanobu Nakayama,[†,‡] Satoshi Goto,[†] Yoshiharu Uchimoto,[†] Masataka Wakihara,*[,†] Yoshinori Kitajima,[§] Takafumi Miyanaga,[∥] and Iwao Watanabe[⊥]

Department of Applied Chemistry, Tokyo Institute of Technology, Ookayama, Meguro-ku, Tokyo 152-8552, Japan, Japan Society for the Promotion of Science, Tokyo, Japan, Photon Factory, Institute of Materials Structure Science, High Energy Accelerator Research Organization, 1-1 Oho, Tsukuba, Ibaraki 305-0801, Japan, Department of Materials Science and Technology, Faculty of Science and Technology, Hirosaki University, Hirosaki, Aomori 036-8561, Japan, and Faculty of Science, Osaka Women's University, 2-1 Daisan-cho, Sakai, Osaka 590-0035, Japan

Received: February 1, 2005; In Final Form: April 7, 2005

Changes in the electronic structure of olivine $Li_{1-x}CoPO_4$, 4.8 V positive electrode material for lithium ion batteries, were investigated using the X-ray absorption spectroscopy (XAS) technique. The threshold energy in the Co K-edge increased with electrochemical Li removal, indicating the oxidation of cobalt ions due to charge compensation. Moreover, P and O K-edge XAS showed a slight shift in threshold energy with Li removal. Although it is generally believed that the electrons of PO_4 polyanion do not contribute to the oxidation process, present experimental results indicate changes in the electronic structure around PO_4 units. Such results would be interpreted by the idea of the hybridization effect between the Co 3d and O 2p orbitals and of the polarization effect introduced by Li ions.

Introduction

The rechargeable lithium ion battery is a device that meets crucial demands of our modern society, acting as the power source of various portable devices, and in the future is expected to be used in electric vehicles, and so on. Thus, high-energy, high-density, low-cost, long-life, and environmentally friendly electrode materials are urgently needed today. Recently, intensive work has been dedicated to the phosphate system $LiMPO_4$ (M = Fe, Ni, Co)[1−4] with olivine-related structures as positive electrodes for rechargeable lithium ion batteries since the first report by Padhi et al.[1] The advantages of utilizing an olivine-type structure come from the following two reasons: (1) these materials have a relatively larger theoretical capacity, ∼170 mAh/g, and a higher voltage, over 4.5 V (in the case of $LiCoPO_4$) versus Li^+/Li, than the layered rocksalt-type $LiCoO_2$ and $LiNiO_2$ and spinel $LiMn_2O_4$ now being commercially used as 4 V positive electrode materials, and (2) recent efforts in improving the electrolyte make it possible to realize stable charge/discharge reactions over 5 V.

Olivine-type $LiMPO_4$ belongs to the space group *Pnma*, and there are four formula units ($Li_4M_4P_4O_{16}$) in its orthorhombic unit cell. The olivine-type structure consists of a hexagonal close-packing (hcp) of oxide ions. Fe and Li ions are located at two kinds of octahedral sites, and MO_6 and LiO_6 octahedrons share their corner and edge, respectively. P ions reside in tetrahedral sites and form compact PO_4 polyanion units (see Figure 1). It was generally recognized that these polyanion units formed their valence and conduction band at a region far from the Fermi level where electronic exchange mainly occurs because of its closed shell electronic configuration. (For example, the main group of metal oxides showed insulating behavior with a large band gap.) In addition, these PO_4 polyanion units form strong covalent bonds. As a result, the valence electrons of transition metals tend to be isolated from those of polyanions, leading to the fact that the electronic exchange arising from Li removal/uptake mainly occurs at transition metal ions. This simple electronic description of $LiMPO_4$ gives us a variety of knowledge on the electrochemical

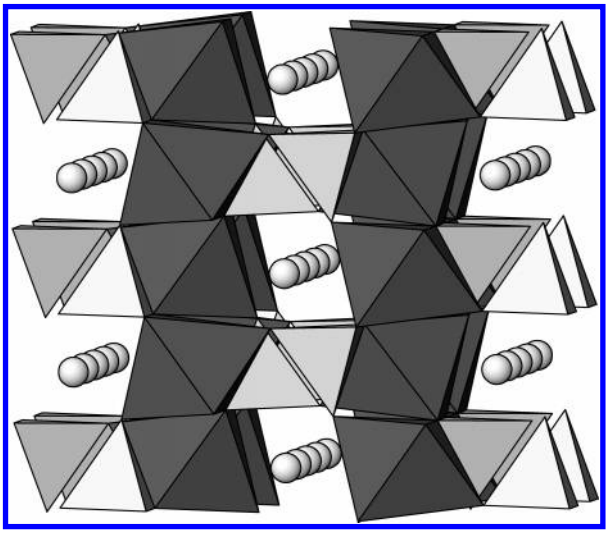

Figure 1. Crystal structure of olivine-type $LiCoPO_4$. The white spheres indicate Li ion, and CoO_6 and PO_4 polyhedrons are represented by darker octahedrons and brighter tetrahedrons, respectively. Crystal structure parameters are referred to Rietveld analysis of the present study (see Table 1).

* Corresponding author. Phone: +81-3-5734-2145. Fax: +81-3-5734-2146.
[†] Tokyo Institute of Technology.
[‡] Japan Society for the Promotion of Science.
[§] Photon Factory.
[∥] Hirosaki University.
[⊥] Osaka Women's University.

10.1021/jp050569s CCC: $30.25
Published on Web 05/14/2005

behavior in this system. For example, the isolated electronic structure of the transition metal would be the reason for the observed high-voltage properties,[1−4] and it simultaneously leads to the low electronic conductivities, causing technical difficulties for battery construction.[4−7] Therefore, an understanding of the unique electronic structure is important in order to utilize it for the rechargeable lithium ion battery.

Quite recently, Zhou et al.[8] and Bacq et al.[9] reported the electronic structure of olivine-type $Li_{1-x}FePO_4$ and $Li_{1-x}CoPO_4$, respectively, by the computational method of density functional theory within the LDA + U approximation. As described in these papers, the LDA + U approximation is essential to recover the experimental results, such as phase stabilization, electrochemical behavior, magnetic structure, and insulating property, because of the strong electron correlation effect. In addition, Bacq et al.[9] argued in their calculation of $Li_{1-x}CoPO_4$ that the Li band strongly hybridized with the PO_4 band, Li removal increases the electronic polarization effect on P, and the wide Co-band structure affects the $(Li)PO_4$ band at the energy state around −8 eV to the Fermi level. That is to say, PO_4 polyanions as well as Co ions vary their electronic structure via the polarization effect during the Li removal/uptake reaction. Simultaneously, we have reported the electronic structure of $Li_{1-x}CoPO_4$ by Co and O K-edge X-ray absorption spectra (XAS),[10] and it was revealed that the electronic structure of oxide ions varied with electrochemical Li extraction, so our experimental observation indicated an agreement with the theoretical work of Bacq et al.[9]

In the present study, to understand the electronic structure and its variation upon Li removal/uptake, a systematic structural study for the $Li_{1-x}CoPO_4$ system has been investigated experimentally using Co, P, and O K-edge XAS.

Experimental Section

The olivine-type $LiCoPO_4$ was synthesized by solid-state reaction. The stoichiometric reagents of Li_2CO_3, $Co(COO)_2 \cdot H_2O$, and $(NH_4)_2HPO_4$ were used as starting materials. The mixtures were heated at 350 °C for 9 h in air, ground in an agate motor, and heated again at 600 °C for 12 h. The phase identification and structural refinement for $LiCoPO_4$ were carried out by the powder X-ray diffraction technique using Cu Kα radiation (RINT-2500V, Rigaku Co., Ltd). The Rietveld method was adopted for the structural refinement using the RIETAN-2000 profile refinement program.[11]

The electrochemical charge/discharge reaction was carried out in the 3.5−5.1 V range at 0.1 mA cm^{-2} using a three-electrode cell. Li foil (Aldrich) was used as the counter and reference electrodes, and a 1 M solution of $LiPF_6$ in anhydrous ethylene carbonate/diethyl carbonate (EC/DEC, 1:1 volume ratio) was used as the electrolyte. The working electrode was a mixture of 70 wt % olivine powders, 25 wt % acetylene black current collector, and 5 wt % poly(tetrafluoroethylene) (PTFE) binder. The phase identification for the samples before and after lithium extraction was carried out by the powder X-ray diffraction (XRD) technique using Cu Kα radiation (RINT-2500V, Rigaku Co., Ltd). The Co, P, and O K-edge XAS measurements were carried out using synchrotron radiation at the beam lines BL-7C, BL-11B, and BL-11A, Photon Factory (PF), High Energy Accelerator Research Organization, in Tsukuba, Japan. The XAS measurement of the Co K-edge was performed by the transmission method, and Cu metal foil was used for the calibration of the absorption energy scale. The absorbance of P and O K-edge spectra was determined by the total-electron-yield method, and the absolute energies were calibrated using S and O K-edge XAS of the S and NiO powder, respectively. For the samples after electrochemical treatment, all installation operations for the Co, P, and O K-edge XAS were performed under an Ar or N_2 atmosphere to prevent the reaction with moisture. In the case of the Co K-edge spectra, we also investigated local structural parameters by means of analyzing extended X-ray absorption fine structure (EXAFS) oscillations. The Co K-edge EXAFS analysis is performed by curve-fitting procedures using REX2000 data analysis software.[12] Theoretical parameters of backscattering factors and phase shifts used in the curve-fitting analysis were calculated by FEFF7 software.[13]

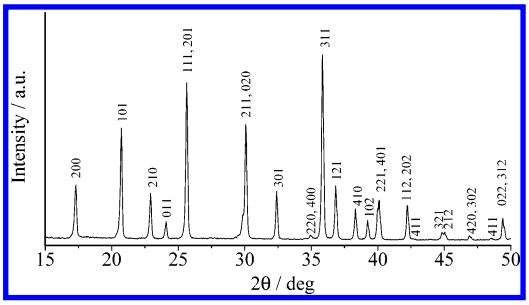

Figure 2. XRD patterns of $LiCoPO_4$.

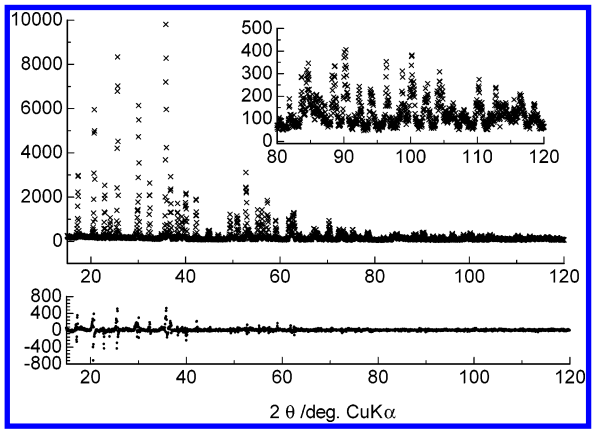

Figure 3. Rietveld refinement patterns for $LiCoPO_4$. The upper panel shows observed (cross) and calculated (gray line) X-ray diffraction patterns, and the lower panel shows the difference between observed and calculated patterns.

Results

Synthesis and Electrochemical Behavior. Figure 2 shows the observed powder XRD pattern of synthesized $LiCoPO_4$. As seen in the figure, all diffraction peaks can be indexed by the orthorhombic system. The results of refinements are listed in Table 1, and Figure 3 shows the final observed, calculated, and difference profiles for the sample. (Note that the Debye−Waller coefficient *B* in Li ion sites was fixed at 1.0 for the Rietveld analysis because of the rather low scattering ability of Li ions, and the common *B* parameter was used for each oxygen site.) Good agreement was obtained with structural parameters reported previously.[14] The important bond lengths and bond valence sums[15] are listed in Table 2. The bond valence sum results indicate that Li, Co, and P have valence states of +1, +2, and +5, respectively.

Figure 4a shows voltage profiles of the first charge/discharge reaction in the $Li_{1-x}CoPO_4$ system, and it was revealed that the Li removal/uptake proceeded reversibly up to ∼120 mAh/g as reported previously.[2] It is noted that the total charge capacity (>180 mAh/g) exceeded the theoretical one (=167 mAh/g), indicating that the reaction includes side reactions to a certain

TABLE 1: Structural Parameters of $LiCoPO_4$ Obtained by the Rietveld Analysis for the XRD Data[a]

$LiCoPO_4$ in *Pnma* (unit cell: $Li_4Co_4P_4O_{16}$, see Figure 1)
lattice parameters: $a = 10.22097(228)$, 5.93228(131), 4.70809(105)
cell volume: $V = 285.469(110)$ Å^3
reliability parameters: $R_{wp} = 10.19\%$, $R_p = 7.49\%$, $S = (R_{wp}/R_e) = 1.6588$

label/atom	site	site occupancy g	x	y	z	B/Å^2
Li1/Li	4a	1.0	0.5	0.5	0.5	1.0
Co1/Co	4c	1.0	0.27895(13)	0.25	0.97861(33)	0.321(40)
P1/P	4c	1.0	0.09391(25)	0.25	0.41649(49)	0.270(60)
O1/O	4c	1.0	0.45385(65)	0.25	0.20860(103)	0.867(70)
O2/O	4c	1.0	0.10080(54)	0.25	0.74557(109)	0.867
O4/O	8d	1.0	0.16710(48)	0.03820(62)	0.27938(71)	0.867

[a] Each refinement quality parameter is defined as follows:

$$R_{wp} = [\sum_i w_i(y_{i,obsd} - y_{i,calcd})^2 / \sum_i w_i y_{i,obsd}]^{1/2}, \quad R_p = \frac{\sum_i |y_i - f_i(x)|}{\sum_i y_i}$$

extent, such as the decomposition of electrolyte solution. However, for convenience, the samples electrochemically prepared were expressed hereinafter by the composition x in $Li_{1-x}CoPO_4$ under the assumption that all the passed currents via the outer circuit were consumed for the Li extraction reaction (or along with Faraday's rule). In detail, two plateaus were observed in the charge process, ~4.8 V ($0 \le x \le$ ~0.3) and ~4.9 V ($x >$ ~0.3), respectively, while the discharge profile showed one voltage plateau at ~4.8 V.[2] Since the initial irreversible capacity roughly coincides with that of the first plateau (~4.8 V), it is conceivable that the first plateau corresponds to the side reaction as mentioned above. However, the charge/discharge behavior in this region (Figure 4b) explicitly showed that the reversible Li removal/uptake reaction preceded in this region. The XRD measurement showed no marked change before and after Li removal (samples with compositions of $x = 0$ and 1), indicating that the framework of the host structure was maintained after Li removal (Figure 5).

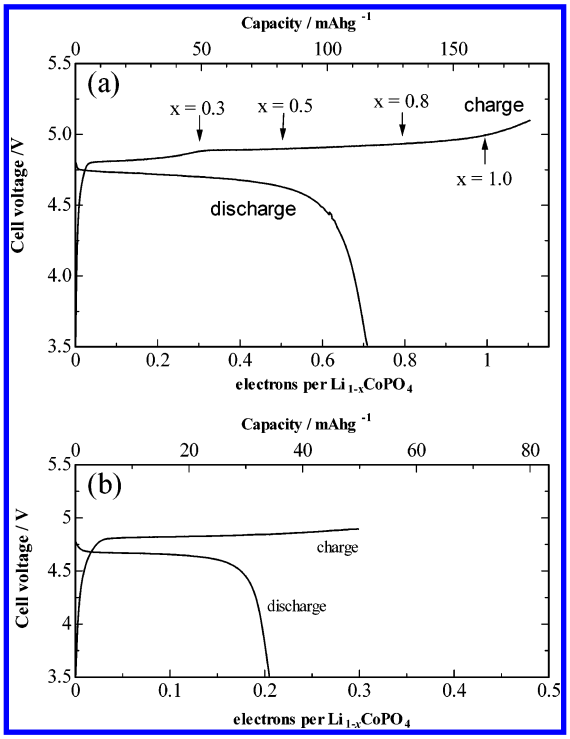

Figure 4. First charge and discharge profiles of $LiCoPO_4$: (a) cutoff, 3.5−5.1 V; (b) cutoff, $x = 0.3$ (charge) and 3.5 V (discharge).

TABLE 2: List of Important Bond Lengths Obtained by Rietveld Analysis (See Table 1)

	bond	bond length/Å	bond valence sum
CoO_6 octahedron	Co−O3 (×2)	2.0265(38)	1.706
1st neighbor ions around Co	Co−O2 (×1)	2.0900(61)	
	Co−O1 (×1)	2.1259(54)	
	Co−O3 (×2)	2.2115(37)	
second and third neighbor	Co−P (×1)	2.2115(37)	
ions around Co ion	Co−Li (×2)	3.2154(13)	
	Co−P (×4)	3.2515(13)	
PO_4 tetrahedron	P−O1 (×1)	1.5480(939)	4.503
	P−O2 (×1)	1.5510(49)	
	P−O3 (×2)	1.5985(42)	
LiO_6 octahedron	Li−O1 (×2)	2.0747(35)	0.987
	Li−O2 (×2)	2.1670(38)	
	Li−O3 (×2)	2.1676(44)	

The results also indicated no marked lattice parameter change because of the rather small shift in 2θ of each peak, and this is consistent with the previous study.[4] In addition, Leyzerovich et al. have recently reported similar electrochemical and structural behavior.[7] They reported that $LiCoPO_4$ synthesized at a high temperature (~800 °C) showed one voltage plateau, and a splitting of diffraction peaks was observed by synchrotron XRD with the progress of charging, indicating the two-phase coexistence reaction. On the other hand, the samples synthesized at a low temperature (~600 °C in argon flow) showed two distinct charge/discharge plateaus, and no evidence of the two-

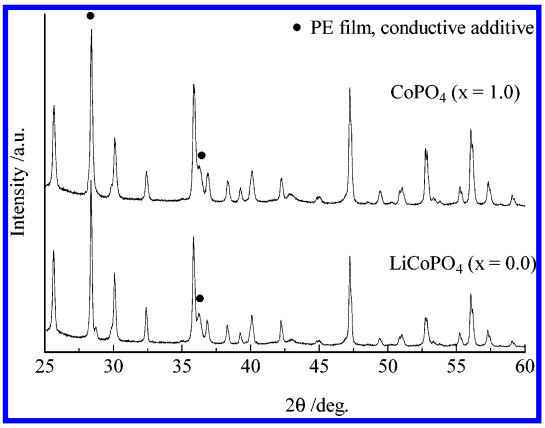

Figure 5. Comparison of the XRD patterns of electrode materials of $LiCoPO_4$ (before charging) and $CoPO_4$ (after charging).

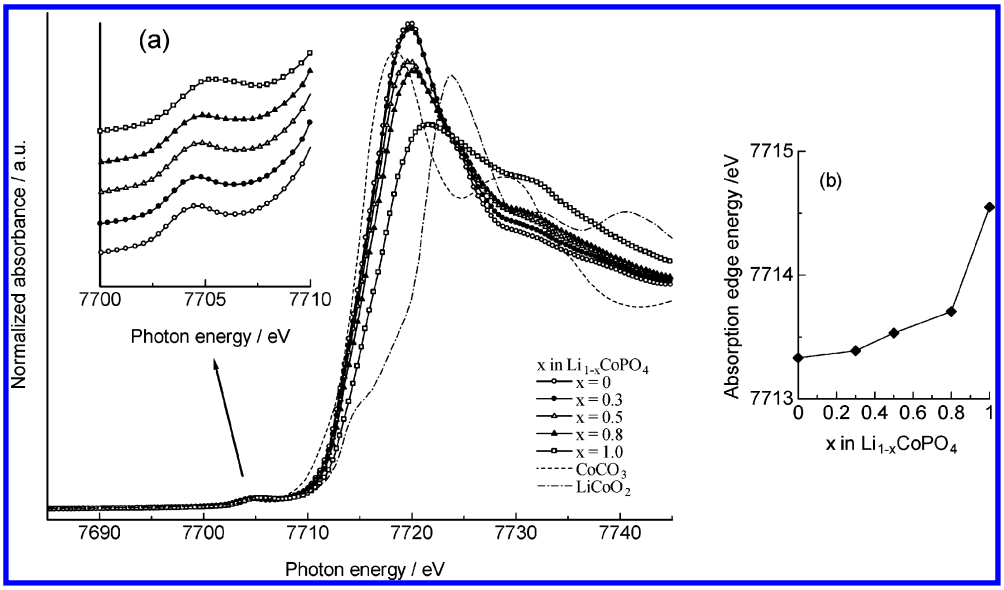

Figure 6. (a) Co K-edge XAS of $Li_{1-x}CoPO_4$ during the lithium extraction process. The inset shows the magnification of the spectra at the pre-edge region. (b) Variation of the absorption edge energy as a function of composition *x*.

phase coexistence reaction was observed in their synchrotron XRD patterns with electrochemical charging. (Note that their report showed amorphization of the electrode material, while no explicit amorphization behavior was observed in our case, as mentioned above.) Thus, our observed two distinct plateaus with electrochemical charging may depend on the low-temperature synthesis condition. The exact reasons for the distinct plateau are still ambiguous; however, there are several plausible reasons, for example, the formation of a superstructure with an ordered arrangement of Li ions or Co^{2+}/Co^{3+} ions in the olivine structure as suggested in spinel $LiMn_2O_4$ (see ref 16 for the Li ordering model and ref 17 for the Mn^{3+}/Mn^{4+} ordering model) and/or the modification of surface structure arising from the difference in synthesis temperature, which may affect the electrochemical overpotential. Further study is needed to understand the double plateau in the voltage diagram.

Co K-Edge XAS. The Co K-edge XAS around threshold energy for electrochemically prepared samples, $Li_{1-x}CoPO_4$, is presented in Figure 6a, and its estimated threshold energy is also shown in Figure 6b as a function of the composition *x*. The spectra of $CoCO_3$ and $LiCoO_2$ as the reference materials of Co^{2+} and Co^{3+} are also shown in Figure 6a. Since the threshold energy of $LiCoPO_4$ is close to that of the divalent reference, $CoCO_3$, Co ions are almost 2+ in valence state in the $LiCoPO_4$, which agrees with the conclusion of bond valence sum obtained by XRD measurement (see Table 2). During the charge reaction, the threshold energy gradually shifted to the higher energy side, indicating that the Co ion is oxidized for the charge compensation in the entire region of the charge reaction (from $x = 0.0$ to $x = 1.0$). Similar results were also reported recently for the samples of the end composition (fully charged and discharged ones).[18]

The local structure of cobalt ions in the olivine-type $Li_{1-x}CoPO_4$ compounds has been quantitatively determined by EXAFS oscillation analysis. Fourier transforms (FTs) of the EXAFS oscillations yield a pseudoradial structure function (RSF) of the local atomic environment around the absorber atom. FTs of the k^3-weighted EXAFS oscillation were calculated in the range from $k = 3$ to $k = 11$ where the EXAFS oscillation is clear enough to neglect the signal/noise error in this *k* region. The RSF of the Co K-edge EXAFS is presented in Figure 7. Three peaks were observed in the whole composition range *x*,

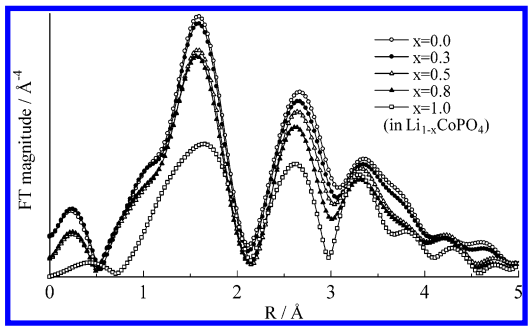

Figure 7. Fourier transformation of Co K-edge EXAFS spectra for $Li_{1-x}CoPO_4$.

indicating the local structural environments around Co ions are roughly maintained during Li extraction, as indicated by the XRD measurements in Figure 5. Each peak of the RSF shown in Figure 7 is assigned by the theoretical simulation of RSF based on the structural parameters (see Table 2) by using FEFF7 sofware.[13] The first peak around 1.4 Å and the second one around 2.6 Å correspond to the Co−O and Co−P interactions, respectively. The third peak around 3.3 Å would be ascribed to the Co−Co interactions; however, a small contribution of the second neighbor Co−O and multiple-scattering effects are conceivable according to the present MS simulation. Therefore, we discuss hereinafter the first Co−O and second Co−P interactions appearing in the RSF diagram. (Note that Co−Li interaction is negligible because of the low backscattering ability of the lithium. In addition, the observed interatomic distance in the figure showed much smaller than the expected one from the data of ionic radii,[19] because phase-shift corrections have not been applied to the RSF diagram.)

In crystallographic view, each peak in the RSF, Co−O and Co−P, consists of several kinds of interactions, as seen in Table 2. Considering the interatomic distance indicated in Table 2, three shell models were adopted for the curve-fitting procedure, 6-coordinated Co−O (∼2.1 Å), 1-coordinated Co−P (∼2.7 Å), and 4-coordinated Co−P (∼3.2 Å) interactions. The best fitting results are compared to the experimental spectra of k^3-weighted EXAFS oscillation in Figure 8, and the fitted structural parameters are summarized in Table 3. The residue increased slightly with Li extraction, and Figure 9 shows the variation of the refined parameters of interatomic distance *R* and Debye−

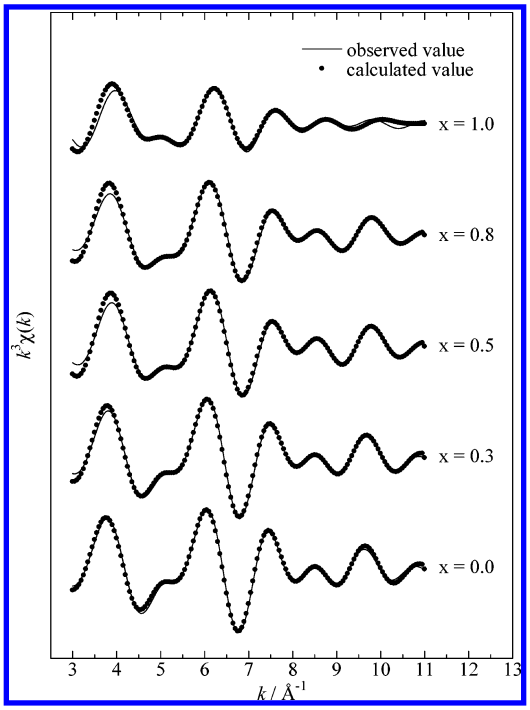

Figure 8. Typical results of the curve-fitting procedure for inverse FT spectra for the Co K-edge XAS of $Li_{1-x}CoPO_4$.

TABLE 3: List of Structural Parameters Determined by Co K-edge EXAFS, Coordination Number CN, Interatomic Distance *r*, and Debye−Waller Factors *σ*, for the Olivine-Type $Li_{1-x}CoPO_4$[a]

	Co−O			Co−P			Co−P			residue/
x	CN	*r*/Å	*σ*/Å	CN	*r*/Å	*σ*/Å	CN	*r*/Å	*σ*/Å	%
0	6[b]	2.067	0.088	1[b]	2.748	0.037	4[b]	3.196	0.042	1.183
0.3	6[b]	2.061	0.091	1[b]	2.749	0.047	4[b]	3.192	0.049	1.025
0.5	6[b]	2.034	0.100	1[b]	2.753	0.063	4[b]	3.173	0.060	2.912
0.8	6[b]	2.034	0.101	1[b]	2.746	0.064	4[b]	3.169	0.069	3.058
1.0	6[b]	2.011	0.136	1[b]	2.715	0.062	4[b]	3.168	0.103	5.832

[a] Residue = $100 \times \sum\{k^n\chi_{obsd}(k) - k^n\chi_{al}(k)\}^2/\sum\{k^n\chi_{obsd}(k)\}^2$. [b] Fixed parameter for the curve-fitting procedure.

Waller factors σ as a function of composition x. As seen in the figure, the interatomic distances for Co−O and Co−P decreased, while the Debye−Waller factors increased with Li extraction. Shrinkage of both interatomic distances corresponds to a decrease in the ionic radii of Co ions arising from oxidization of Co ions from +2 to +3. However, the decrease in interatomic distance is relatively smaller than the one expected in quantitative aspect. (Only an ∼0.06 Å decrease in interatomic distance of Co−O was observed for the samples between $LiCoPO_4$ and $CoPO_4$.) One conceivable reason is that the spin configuration around Co ions changed from low-spin (for Co^{2+}) to high-spin (for Co^{3+}) configuration. In this case, the shrinkage of ionic radii is close to our EXAFS analysis (decrease of ∼0.04 Å expected according to the list of Shannon's ionic radii (Co^{2+} (low spin) 0.65 Å and Co^{3+} (high spin) 0.61 Å for a 6-coordinated environment). However, Okada et al. have reported the low-spin configuration of the Co^{3+} ion after Li extraction using measurement of magnetism.[18] The inset of Figure 6a shows the magnification of the pre-edge XAS peaks observed in the Co K-edge, which represent the transition of the 1s electron to an unoccupied 3d orbital of the Co ion. (Although the s → d transition is prohibited according to the dipole transition rule, a slight distortion in the CoO_6 octahedron and overlap of the O 2p orbital with the Co d band cause the weak absorption peak.) No marked change in the peak feature

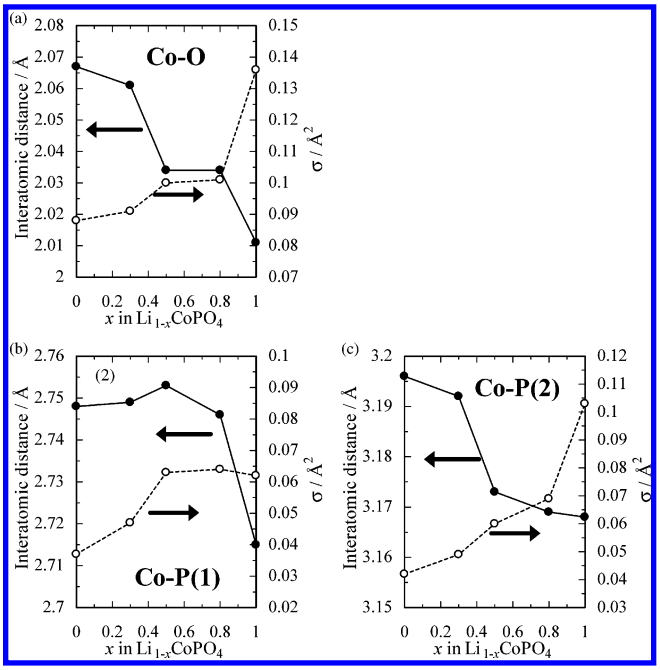

Figure 9. Compositional dependence of changes in interatomic distance and Debye−Waller coefficients in $Li_{1-x}CoPO_4$ obtained by Co K-edge EXAFS analysis for (a) first neighbor interaction of Co−O, (b) second neighbor interaction of Co−P, and (c) third neighbor interaction of Co−P. The solid and open symbols show the interatomic distance and Debye−Waller coefficients, respectively.

with various lithium concentrations was observed in pre-edge Co XAS. Thus, these experimental results could not positively support our speculation mentioned above. Nevertheless, the rather small volume change before and after Li extraction (in ref 4) would correspond to the not marked change in bond length of Co−O indicated by EXAFS analysis. Further study is required to clarify the small volume change reaction.

The Debye−Waller factor σ of each bond was gradually increased at the composition $0 \le x \le 0.8$, and then, abrupt increase in Co−O and second Co−P interatomic distances was observed at the composition $x > 0.8$, as shown in the RDF signal (Figure 7). Since the electrochemically delithiated samples were thermodynamically metastable, the increase in the Debye−Waller factor would imply the structural distortion, and it would be arising from instability of the delithiated structure.

P and O K-Edge XAS. The variation of P and O K-edge XAS upon lithium extraction reaction in $Li_{1-x}CoPO_4$ was investigated and shown in Figures 10 and 11, respectively.

As seen in Figure 10, one sharp peak A and shoulder B were observed in P K-edge XAS of parent $LiCoPO_4$ material. Peak A gradually shifted with electrochemical Li removal, causing an ∼0.2 eV shift at the composition $x = 1.0$. This indicates that the phosphate ion also contributed to the variation of the electronic structure and became more positive with charging. Nevertheless, the present results indicated the electronic exchange around P ions. Shoulder B also disappeared with lithium removal, and the exact reason for this behavior is still uncertain. Usually, these shoulders following the absorption peak near the edge energy are strongly affected by the local structural distortion around X-ray absorbed ions. Hence, it was speculated that the disappearance of shoulder B can be ascribed to the distortion of PO_4 polyanion structure as observed in Co K-edge XAS. Further discussion on this issue is required, such as the spectral peak assignment by theoretical treatment using multiple-scattering theory.

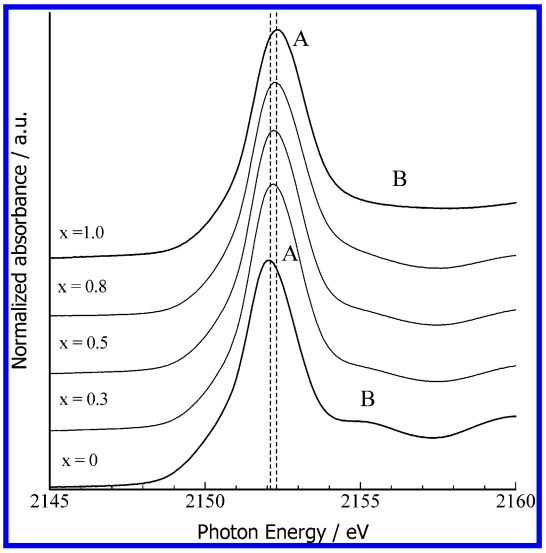

Figure 10. P K-edge XAS of $Li_{1-x}CoPO_4$ during the lithium extraction process.

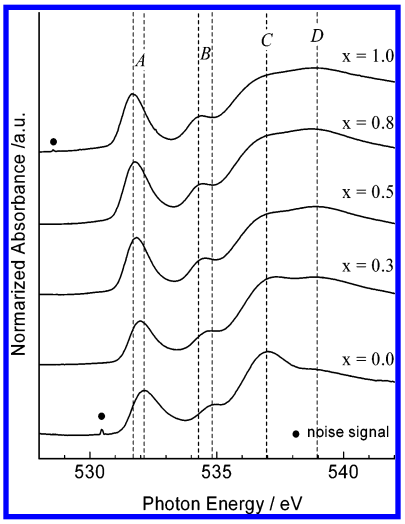

Figure 11. O K-edge XAS of $Li_{1-x}CoPO_4$ during the lithium extraction process.

The O K-edge XAS of $Li_{1-x}CoPO_4$ was also investigated, and the results are shown in Figure 11. Four peaks labeled *A*−*D* were observed in the energy range from 530 to 540 eV. Since the sharp XAS peaks at the lower energy side in transition metal oxides are usually ascribed to the hybrid unoccupied orbital between transition metal d and oxygen 2p orbitals, peak *A* in Figure 11 corresponds to the Co 3d/O 2p hybridized orbital. The broad peaks *C* and *D* would be ascribed to the unoccupied O 2p orbital hybridized with the s and/or p character orbital of P and Co ions. (The origin of peak B is uncertain. However, it is speculated that peak *B* is ascribed to the Co 3d/O 2p hybridized orbital, because the spectral behavior with composition *x* is close to that of peak *A*, and the split in energy between peak *A* and *B* is about 3 eV, which is a typical value of d orbital split in the crystal field.) The whole spectral feature was kept during lithium extraction, so that the crystal structure and local atomic arrangement remains unchanged as indicated in Co K-edge XAS. In addition, the sharp peak feature in peak *A*, which indicates the localized band nature of Co 3d/O 2p, also does not vary with Li extraction. The peaks *A* and *B* gradually shifted to the lower energy side at the early stage of lithium extraction ($0 \leq x \leq \sim 0.5$). Furthermore, the intensity of peak *A* increased with composition *x*, indicating an increase of the hole state at the oxygen site. In other words, the observed peak shift and increase in peak *A* intensity indicate a decrease in d electron donation from transition metal ion to hybridized orbital, as mentioned above. Summing up the discussion, the compositional variations of peak *A* (and maybe peak *B*) would be ascribed to the electronic exchange via hybridized orbital in Co 3d and O 2p during the electrochemical reaction. In addition, only a little variation was observed at O K-edge XAS in the region of $x > \sim 0.5$, which is a one-to-one correspondence observed in Co K-edge XAS. Therefore, the oxide ion only contributed to the charge compensation process at the early stage of lithium extraction, while the cobalt ion did so at the later stage of the reaction. Note that the observed spectral behavior also verifies that the reaction proceeds in the solid-solution manner indicated in ref 7. The assignment of peaks *C* and *D* is difficult, because these peaks include Co and P metal orbital hybridization and the potential effect of ions relatively distant from the ions that absorbed X-rays. The intensity of peak *D* is significantly increased at the first plateau region (∼4.8 V). The origin of this spectral change is uncertain yet, and further studies are required to understand the electronic structural change during the lithium extraction at the first voltage plateau.

Discussion

The present XAS study for $Li_{1-x}CoPO_4$ explicitly revealed that the electronic structures of P and O were varied as well as Co ions with electrochemical charging, and this result seems to be consistent with the reported ab initio study by Bacq et al.[9] Such a behavior of the structural changes in P and O electrons is surprising, since it is generally believed that the energy levels of PO_4 polyanions are apart from the Fermi level where electron transfer occurs. From the analysis of XAS for $Li_{1-x}CoPO_4$ and ab initio study by Bacq et al.,[9] two effects would contribute to the modification of electronic structure in PO_4 polyanions: (1) the hybridization effect between the Co 3d and O 2p orbitals and (2) the polarization effect induced by the strong ionic character of Li ions.

The former effect is clarified by the changes in the pre-edge peak of O K-edge XAS which stems from the hybridization orbital of the Co 3d and O 2p orbitals, indicating that the Co 3d/O 2p hybridized orbital plays an important role during the electrochemical reaction. In addition, one-to-one correspondence was observed in the present Co and O K-edge XAS, as mentioned above, indicating the O 2p electrons contributed to the charge compensation during the electrochemical reaction as well as Co ions. Therefore, our experimental results explicitly showed that the electronic transfer occurs at the Co and O hybridized orbital, even though the valence electrons around Co ions are isolated by the strong covalent bond formation in the polyanion of PO_4. Such an experimental indication agrees well with a previous ab initio calculation using the LDA + U approach by Bacq et al.[9] that the Co band affects the (Li)PO_4 valence band, causing the charge donation from the Co ion to the PO_4 polyanion. Accordingly, it is concluded that the electronic transfer occurred via a hybridized orbital between Co 3d and O 2p during the Li extraction reaction.

On the other hand, the second effect of polarization would also be conceivable according to the ab initio results that the valence orbital of PO_4 located at a lower energy level from the Fermi energy strongly correlated to that of Li.[9] Since the strong ionic character of lithium ions causes the polarization of PO_4 electrons in Li−O−P sequence, the electrons around P ions shift toward the oxygen. Such a polarization effect decreases with Li extraction, and P ions are expected to be more negative than

fully lithiated olivine. This indication of the polarizing effect also agrees with another previous report. Van der Ven et al.[20] showed that the screening effect of oxide ions and electron transfer from lithium ions to neighboring oxide ions lead to effective neutralization of the strong ionic character of Li ions using an ab initio calculation for $LiCoO_2$ electrode material, and we recently demonstrated the electronic interaction between Li and oxide by a combination of experimental XAS and ab initio computation for A-site deficient perovskite materials.[21] Therefore, the shift observed in P K-edge XAS is attributed to the polarization effect caused by lithium ions. Summing up this discussion, the variation of the Co, P, and O K-edge XAS can be understood by the concept of the hybridization between Co and O and of the polarization in Li−O−P sequences.

Acknowledgment. This work was supported by Grant-in-Aid for Scientific Research (no. 16350109) from Ministry of Education, Culture, Sports, Science and Technology. M.N. acknowledges the Japan Society for the Promotion of Science for financial support. XAS measurement has been performed under the approval of the Photon Factory Program Advisory Committee (Proposal Nos. 2003G260, 2003G262, and 2004G288).

References and Notes

(1) Padhi, A. K.; Nanjundaswamy, K. S.; Goodenough, J. B. *J. Electrochem. Soc.* **1997**, *144*, 1188. Padhi, A. K.; Najundaswamy, K. S.; Masquelier, C.; Okada, S.; Goodenough, J. B. *J. Electrochem. Soc.* **1997**, *144*, 1609.

(2) Okada, S.; Sawa, S.; Egashira, M.; Yamaki, J.; Tabuchi, M.; Kageyama, H.; Konishi, T.; Yoshino, A. *J. Power Sources* **2001**, *97*−*98*, 430.

(3) Yamada, A.; Hosoya, M.; Chung, S.-C.; Kudo, Y.; Hinokuma, K.; Liu, K.-Y.; Nishi, Y. *J. Power Sources* **2003**, *119*−*121*, 232.

(4) Amine, K.; Yasuda, H.; Yamachi, M. *Electrochem. Solid-State Lett.* **2000**, *3*, 178.

(5) Yang, S.; Song, Y.; Zavalij, P. Y.; Whittingham, M. S. *Electrochem. Commun.* **2002**, *4*, 239.

(6) Chung, S.-Y.; Bloking, J.-T.; Chiang, Y.-M. *Nat. Mater.* **2002**, *1*, 123.

(7) Leyzerovich, N. N.; Bramnik, K. G.; Baehtz, C.; Buhrmester, T. *Extended Abstracts for Lithium Battery Discussion Electrode Materials*; Bordeaux, France, 2003; N7.

(8) Zhou, F.; Marianetti, C. A.; Cococcioni, M.; Morgan, D.; Ceder, G. *Phys. Rev. B* **2004**, *69*, 201101.

(9) Bacq, O. L.; Pasturel; Bengone, O. A. *Phys. Rev. B* **2004**, *69*, 245107.

(10) Nakayama, M.; Goto, S.; Uchimoto, Y.; Wakihara, M.; Kitajima Y. *Chem. Mater.* **2004**, *16*, 3399.

(11) Izumi, F.; Ikeda, F. *Mater. Sci. Forum* **2000**, *321*−*324*, 198.

(12) RIGAKU EXAFS analysis software, REX2000; Catalogue No. 2612S311/312/321/322, Rigaku Co., 2000.

(13) Multiple-scattering XAS simulation code: Ankudinov, A. L.; Ravel, B.; Rehr, J. J.; Conradson, S. D. *Phys. Rev. B* **1998**, *58*, 7565. Ankudinov A. L.; Rehr, J. J. *Phys. Rev. B* **1997**, *56*, R1712. Zabinsky, S. I.; Rehr, J. J.; Ankudinov, A.; Albers, R. C.; Eller, M. J. *Phys. Rev. B* **1995**, *52*, 2995. For further details, see, for example, the documentation at the following URL: http://leonardo.phys.washington.edu/feff/.

(14) Kubel, F. *Z. Kristallogr.* **1994**, *209*, 755.

(15) Brown, I. D.; ltermatt, D. *Acta Crystallogr.* **1985**, *B41*, 244.

(16) Gao, Y.; Reimers, J. N.; Dahn, J. R. *Phys. Rev. B* **1996**, *54*, 3878. Wong, W. C.; Newman, J. *J. Electrochem. Soc.* **2002**, *149*, A493.

(17) Björk, H.; Gustafsson, T.; Thomas, J. O.; Lidin S.; Petřiček, V. *J. Mater. Chem.* **2003**, *13*, 585.

(18) Okada, S.; Sawa, S.; Uebou, Y.; Egashira, M.; Yamaki, J.; Tabuchi, M.; Kobayashi, H.; Fukumi, K.; Kageyama, H. *Electrochemistry* **2003**, *71*, 1136.

(19) Shannon, R. D. *Acta Crystallogr.* **1976**, *A32*, 751.

(20) Van der Ven, A.; Aydinol, M. K.; Ceder, G. *Phys. Rev. B* **1998**, *58*, 2975.

(21) Nakayama, M.; Imaki, K.; Ra, W.; Ikuta, H.; Uchimoto, Y.; Wakihara, M. *Chem. Mater.* **2003**, *15*, 1728. Nakayama, M.; Ra, W.; Ikuta, H.; Uchimoto, Y.; Wakihara, M. *Electrochemistry* **2003**, *71*, 1025. Imaki, K.; Nakayama, M.; Uchimoto, Y.; Wakihara, M. *Solid State Ionics* **2004**, 172, 73. Nakayama, M.; Imaki, K.; Uchimoto, Y.; Wakihara, M. *Solid State Ionics* **2004**, *172*, 77. Nakayama, M.; Usui, T.; Uchimoto, Y.; Wakihara, M.; Yamamoto, M. *J. Phys. Chem. B* **2005**, *109*, 4135.